Superheavy Hydrogen ^{5}H

A. A. Korsheninnikov,* M. S. Golovkov,*,† and I. Tanihata

RIKEN, Hirosawa 2-1, Wako, Saitama 351-0198, Japan

A. M. Rodin, A. S. Fomichev, S. I. Sidorchuk, S. V. Stepantsov, M. L. Chelnokov, V. A. Gorshkov,
D. D. Bogdanov, R. Wolski,‡ G. M. Ter-Akopian, and Yu. Ts. Oganessian

JINR, 141980 Dubna, Moscow region, Russia

W. Mittig, P. Roussel-Chomaz, and H. Savajols

GANIL BP 5027, F-14076 CAEN cedex 5, France

E. A. Kuzmin, E. Yu. Nikolskii,§ and A. A. Ogloblin

Kurchatov Institute, Kurchatov square 1, 123182 Moscow, Russia

Experimental search for ^{5}H using a secondary beam of ^{6}He has been performed. The transfer reaction ^{1}H(^{6}He, ^{2}He)^{5}H was studied by detecting two protons emitted from the decay of ^{2}He. A peak consistent with a ^{5}H resonance at 1.7 ± 0.3 MeV above the $n + n + t$ threshold was observed, with a width of 1.9 ± 0.4 MeV. The angular distribution of the ^{1}H(^{6}He, ^{2}He)^{5}H reaction was measured as well as the energy correlation of the two protons.

The very neutron rich nucleus ^{5}H having an extreme fraction of neutrons, $N/Z = 4$, was the object of research for more than 40 years. Numerous earliest experiments attempted to observe a particle-stable ^{5}H, either by its beta activity or by direct detection of ^{5}H, finally providing the proof of its instability. Later experiments [1–3] aimed for unbound ^{5}H. However, until now the existence of ^{5}H resonance remains unclear.

In Ref. [1] the $t(t, p)^5$H reaction was studied and a peak at 1.8 MeV relative to the $t + n + n$ threshold was observed. However, since the energy of the tritium beam was low, the authors did not exclude the possibility that this peak can be attributed to a phase space effect. In Ref. [2] the reactions initiated by the pion absorption on a ^{9}Be target were studied using a two-arm spectrometer for detection of two particle coincidences. In the reaction ^{9}Be(π^-, pt)^{5}H a bump at ~ 7 MeV was observed, but another reaction channel, ^{9}Be(π^-, dd)^{5}H, provided no evidence for production of ^{5}H. A bump at different energy of ~ 5 MeV was reported in Ref. [3], where the ^{7}Li(^{6}Li, ^{8}B)^{5}H reaction was studied.

Oscillator shell model calculations of ^{5}H were performed in Ref. [4]. Recently, ^{5}H was calculated as an unstable resonance in the K-harmonics method [5] and in the generator coordinate method [6]. These calculations predict the ^{5}H ground state $1/2^+$ at the energy $E_{^5H} \sim 2.5$–3 MeV above the $t + n + n$ threshold. Also excited states $5/2^+$ and $3/2^+$ were predicted in the region of $E_{^5H} \sim 4.5$–7.5 MeV [4,5].

In the present paper, we report on an experimental study of ^{5}H. We applied a technique that reminds one of the missing-mass method, but with detection of an unstable recoil nucleus. In standard missing-mass experiments the binary reaction $A(b, c)D$ is studied, and by detecting nucleus c, one obtains the excitation energy spectrum of the residual system D. Generally speaking, the more neutron rich system D we want to study, the more proton rich nucleus c has to be detected. As a result, the nucleus c can be even unstable, as, e.g., ^{6}Be, that decays into $p + p + \alpha$, or as singlet state ^{2}He, that decays into $p + p$. Nevertheless, we can deal with the unstable nucleus c, if all particles from its decay are detected. Having kinematically complete information on the unstable system c, we can reconstruct the excitation energy in the residual nucleus D and can perform its spectroscopy.

The reaction $p(^6$He, ^{2}He)^{5}H was chosen for the search for ^{5}H. It is reasonable to expect that neutrons in the ground state of ^{5}H occupy the same orbitals as in ^{6}He. Hence, by the pickup of one proton from ^{6}He, we should selectively populate the ground state $1/2^+$ of ^{5}H. In other interesting reactions, such as $t(t, p)^5$H and $t(^6$He, ^{4}He)^{5}H, the two-neutron transfer is expected to populate also excited states $5/2^+$ and $3/2^+$, which are predicted by the theoretical calculations [4,5]. These broad excited states will render more difficult, if not impossible, the identification of the ground state.

To detect all particles from the decay of the unstable recoil system c in the reaction $A(b, c)D$, we built the RIKEN telescope (Fig. 1), a stack of solid state strip detectors. This telescope allows us to measure angles, energy losses, and energies of several particles detected in coincidence. The detectors have an annular hole for the beam. With this geometry decay products of the system c can be detected at small angles in the laboratory system in inverse kinematics typical for many experiments with secondary beams.
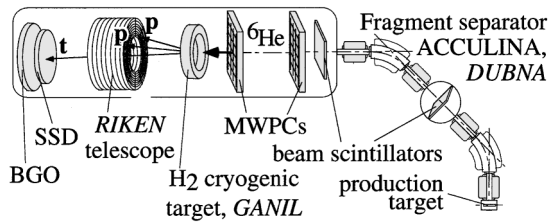
FIG. 1.   Scheme of the experimental setup.

The experimental setup is shown in Fig. 1. The secondary beam of ^{6}He at 36A MeV with the intensity of $\sim 3 \times 10^4$ pps was obtained using the fragment separator ACCULINA at JINR (Dubna). Two plastic scintillators were used for the identification of each particle of the secondary beam and for the measurement of its energy by time of flight. The trajectory of ^{6}He was measured by two multiwire proportional chambers. We used a cryogenic target from GANIL (France), which was filled with hydrogen gas at a temperature of 35 K and pressure of 10 atm. The target thickness was 6×10^{21} protons/cm^2. The two protons originating from the decay of ^{2}He were detected in coincidence by the RIKEN telescope in the energy range of $5.5 \leq E_p^{\text{lab}} \leq 30$ MeV and at angles of $9° \leq \theta_p^{\text{lab}} \leq 22°$. It corresponds to the emission of ^{2}He at small c.m. angles in the $(p, {}^2\text{He})$ reaction, where the cross section should be maximal. Besides protons, we also detected tritons from the decay $^5\text{H} \rightarrow t + n + n$, using a downstream telescope, which consisted of a large-area SSD detector and a BGO crystal and which covered angles $\theta_t^{\text{lab}} \leq 7°$. The keystone of this experiment was the combination of the exotic ^{6}He beam, the hydrogen cryogenic target, and the detection system based on the RIKEN telescope.

Figure 2 shows the obtained ^{5}H spectrum extracted from the $p + p$ coincidences, $p(^6\text{He}, pp)$. The spectrum is shown as a function of energy above the $t + n + n$ threshold. The cutoff at ~ 7 MeV reflects the detection limit due to the RIKEN telescope. The solid histogram shows the result obtained with the hydrogen target. The dashed histogram presents the normalized background obtained with
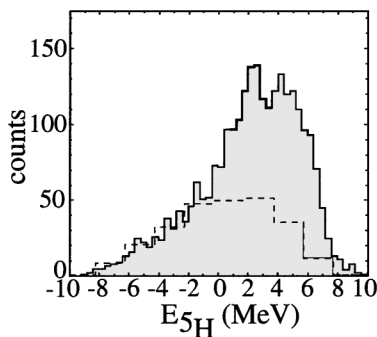
an empty target. This background accounts for events at negative energies in Fig. 2, where ^{5}H would be bound.

Figure 3 shows the ^{5}H spectrum measured in coincidence with triton from the decay of the residual ^{5}H system. This additional coincidence with triton eliminates the background from the empty target measurement, where only two events were detected near zero energy. The spectrum in Fig. 3 shows clearly a peak at ~ 2 MeV, already apparent in Fig. 2. The experimental resolution in these spectra was 1.3 MeV (FWHM).
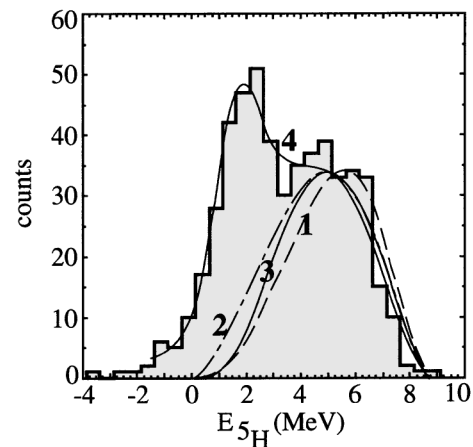
In Fig. 4 the detection efficiency for events measured in the $p + p + t$ coincidence is shown. Since this distribution is smooth at ~ 2 MeV, the detection efficiency cannot be responsible for the 2-MeV peak in the ^{5}H spectrum in Fig. 3. The same is true for $p + p$ coincidence in Fig. 2.

Besides ^{5}H, we simultaneously measured spectra in other reaction channels, $p(^6\text{He}, pt)^3\text{H}$ and $p(^6\text{He}, t)^4\text{He}$. These spectra show well-defined peaks corresponding to the residual nuclei ^{3}H and ^{4}He, and confirm the reliability of the results obtained.

We expected that in the reaction $p(^6\text{He}, pp)$ two protons would be produced in the virtual singlet state ^{2}He. Figure 5 shows that it is really true. This figure presents the distribution of the two protons as a function of their relative energy $E_{p\text{-}p}$. In this case the detection efficiency has a shape of a bump with maximum at $E_{p\text{-}p} \sim 2.5$ MeV, and we show in Fig. 5 the spectrum corrected by detection efficiency. The shape of the experimental spectrum is in perfect agreement with the calculations of the virtual singlet state ^{2}He, which are shown by curves in Fig. 5 and which were obtained as follows. The relative energy spectrum

$$dN/dE_{p\text{-}p} \propto \sqrt{E_{p\text{-}p}} \sqrt{E_{\text{cm}} - E_{p\text{-}p} - E_{^5\text{H}}} |M|^2 \quad (1)$$

was calculated with the matrix element determined by the phase shift known from the Landau-Smorodinskii's effective range approximation for two protons with the scattering length $a_{pp} = -7.806$ fm [7]. The experimental

FIG. 2.   Spectrum of ^{5}H from the reaction $p(^6\text{He}, pp)$. Dashed histogram shows the empty-target background.

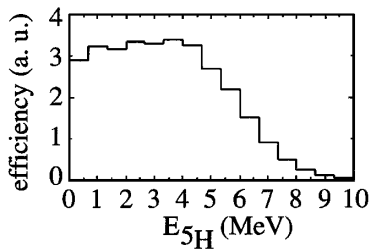FIG. 3.   Spectrum of ^{5}H from the reaction $p(^6\text{He}, ppt)$. Curves show calculations explained in the text.

FIG. 4.   Detection efficiency for the ^{5}H spectrum measured in $p + p + t$ coincidence.

spectrum in Fig. 5 contains events with energy $E_{^5H}$ up to 7 MeV. Therefore, Eq. (1) was integrated in the same way. The obtained result is shown in Fig. 5 by the solid curve. The dashed curve was calculated using the phase shift found from the solution of the Schrödinger equation with the Coulomb interaction and simple nuclear potential of the Gaussian shape [8].

Returning to the spectrum in Fig. 3, we investigated various kinds of $t + n + n$ continuum. The simplest evaluation of the continuum is the three-body phase volume, $dN/dE_{^5H} \propto E_{^5H}^2$. This was incorporated into the Monte Carlo simulation of measurement, and the obtained result is shown in Fig. 3 by curve 1, which evidently cannot account for the peak at 2 MeV.

Curve 2 in Fig. 3 corresponds to the $n + n$ final state interaction. Starting from the effective range approximation for two neutrons [7], one can easily obtain the matrix element $|A|^2 \propto 1/(0.12 + E_{n\text{-}n}[\text{MeV}])$, where the value 0.12 MeV corresponds to the scattering length $a_{nn} = -18.5$ fm. We obtain the three-body continuum with the $n + n$ final state interaction

$$dN/dE_{^5H} \propto \int_0^{E_{^5H}} \sqrt{E_{n\text{-}n}(E_{^5H} - E_{n\text{-}n})}\,|A|^2\,dE_{n\text{-}n}$$
$$\propto E_{^5H}[1/2 + \beta - \sqrt{\beta(1 + \beta)}\,], \qquad (2)$$

where $\beta = 0.12/E_{^5H}[\text{MeV}]$. Curve 2 in Fig. 3 was obtained after incorporating Eq. (2) into the Monte Carlo simulation of the experiment. Not shown here is the influence of the $n + t$-final state interaction; it gives a distribution which does not differ much from curves 1–3 in Fig. 3. Besides, we investigated all final state interactions
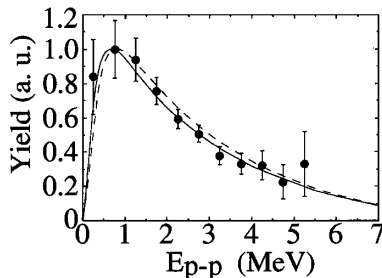

FIG. 5.   Relative energy distribution of two protons from the reaction $p(^6\text{He}, ppt)$. Curves show calculations of the singlet state ^{2}He.

involving the detected proton(s). These processes cannot account for the peak at 2 MeV also.

Curve 3 in Fig. 3 shows the continuum which reflects the initial state effect. The projectile ^{6}He is known as a nucleus of unique structure. It has a two-neutron halo, where the valence neutrons form the exotic dineutron and cigar-like configurations. We evaluated the influence of the ^{6}He structure on the ^{5}H spectrum in the sudden approximation, using the ^{6}He wave function calculated in the $\alpha + n + n$ model in the K-harmonics method [9].

This wave function in the momentum space has the form $\Phi(\text{æ}, \Omega_5) = \sum \chi_{KLS}^{ll}(\text{æ})[Y_{KLM}^{ll}(\Omega_5)\Theta_{SM'}]_{J=0}$. Here the functions Y_{KLM}^{ll} and $\Theta_{SM'}$ are known, while the functions $\chi_{KLS}^{ll}(\text{æ}) = i^K/\text{æ}^2 \int \chi_{KLS}^{ll}(\rho)J_{K+2}(\text{æ}\rho)\rho^{1/2}\,d\rho$ are determined by the hyper-radial functions $\chi_{KLS}^{ll}(\rho)$, which were calculated in Ref. [9] in numerical form. The momentum æ is connected with the total energy in the three-body system, $\text{æ} = \sqrt{2mE}/\hbar$; Ω_5 are the hyperspherical variables connected with the Jacobi momenta (other notations, see in [9]). Since an element of volume in the momentum space is $d\tau = \text{æ}^5 d\text{æ} d\Omega_5$, we obtain the following distribution of energy in ^{6}He, $dN/dE \propto \int |\Phi(\text{æ}, \Omega_5)|^2 \text{æ}^4\,d\Omega_5 = \sum |\chi_{KLS}^{ll}(\text{æ})|^2 \text{æ}^4$. When calculating curve 3 in Fig. 3, we used the main components with hypermomentum $K = 2$, which has a weight of 92%. In this case

$$dN/dE \propto (|\chi_{200}^{00}(\text{æ})|^2 + |\chi_{211}^{11}(\text{æ})|^2)\text{æ}^4. \qquad (3)$$

Similar to curves 1 and 2, curve 3 in Fig. 3 does not account for the 2-MeV peak. Thus, the exotic structure of the initial nucleus ^{6}He is not responsible for this peak. The internal motion in ^{6}He is characterized by a rather broad distribution, and Eq. (3) has a maximum at ~13 MeV and a FWHM ~25 MeV.

Consequently, we interpret the 2-MeV peak in Fig. 3 as a resonance ^{5}H. In order to determine its energy and width, we fitted the spectrum combining each of the curves 1–3 with the Breit-Wigner formula for the 2-MeV peak folded with the experimental resolution. The performed fits give the following parameters of ^{5}H, $E^{\text{obs}} = 1.7 \pm 0.3$ MeV and $\Gamma^{\text{obs}} = 1.9 \pm 0.4$ MeV. Fitting with formulas that include the correct threshold behavior give identical results within the quoted precision. Curve 4 in Fig. 3 shows a typical example of these fits.

Since we measured the angles and energy of each proton from the decay of ^{2}He, the motion of the center of mass of ^{2}He is known, and we can extract the angular distribution of the reaction ^{6}He(p, ^{2}He)^{5}H. It is shown in Fig. 6 for events from the 2-MeV peak in Fig. 3. The shape of this angular distribution corresponds to the angular momentum transfer $l = 0$. This is what is expected for the population of ^{5}H$_{\text{gs}}(1/2^+)$.

The absolute value of the cross section is rather low. For example, in Fig. 6 we show the results of distorted-wave Born approximation (DWBA) calculations. Curve 1
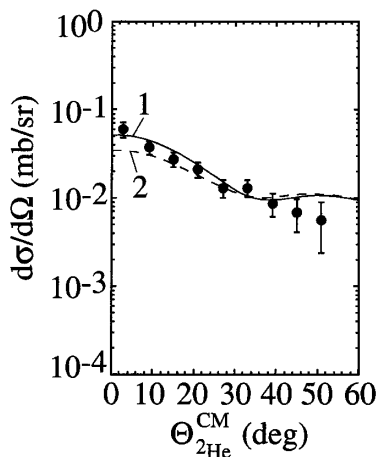
FIG. 6.   Cross section of the reaction ^{6}He$(p, ^2$He$)^5$H. Curves show the DWBA calculations normalized to the experiment.

was obtained with the optical potential parameters for the $p + {}^{14}$C and $d + {}^{12}$C scattering tabulated in Ref. [10]. Curve 2 was calculated using parameters from the ^{4}He$(p, d)^3$He reaction [11]. The shapes of these curves are in satisfactory agreement with the experiment. The absolute values of calculated cross sections are not well defined, because of ambiguity of the form factor of ^{2}He. However, in general, the calculated cross sections have to be reduced by about 1 order of magnitude for normalization to the experimental data in Fig. 6. Most likely, this reduction reflects scattering on two valence neutrons of ^{6}He. Namely, to populate ^{5}H$(1/2^+)$, the incoming proton must pick up another proton from the α core in ^{6}He, while the valence neutrons should not be scattered. Such a rescattering takes place in the nuclear well, and the corresponding theoretical investigation would be desirable.

The observed peak in Fig. 3 at $E^{\mathrm{obs}} = 1.7 \pm 0.3$ MeV is close to one reported in Ref. [1]. A bump at a higher energy of ~ 5–7 MeV observed in Refs. [2] and [3] can reflect the excited states of ^{5}H $5/2^+$ and $3/2^+$, as argued in Ref. [5]. In the latter paper the theoretical calculation of resonance ^{5}H was performed and the ground state of ^{5}H was found at ~ 2.5 MeV. At the present stage of calculations this result can be considered as consistent with our observation.

Our peak of ^{5}H at 1.7 ± 0.3 MeV being located lower than ^{4}H [12] is qualitatively consistent with a pairing of

two outer neutrons in ^{5}H. At last, according to the known systematic for helium isotopes, where ^{8}He is more bound than ^{6}He, and ^{7}He has lower energy above threshold than ^{5}He, the characteristics observed for ^{5}H suggest that ^{7}H may exist as a low lying resonance and make studies of ^{7}H especially interesting.

Summarizing, we investigated the transfer reaction $p(^6$He$, ^2$He$)^5$H by detecting the two protons emitted from the decay of ^{2}He and observed a peak which we interpret as a resonance ^{5}H with parameters of $E^{\mathrm{obs}} = 1.7 \pm 0.3$ MeV and $\Gamma^{\mathrm{obs}} = 1.9 \pm 0.4$ MeV. The angular distribution of the $p(^6$He$, ^2$He$)^5$H reaction was measured as well as the energy correlation of two protons. The former has a shape consistent with the angular momentum transfer $l = 0$ expected for the population of ^{5}H$_{\mathrm{gs}}(1/2^+)$, while the latter confirms the emission of the ^{2}He virtual state in the reaction studied.

*On leave from the Kurchatov Institute, Kurchatov square 1, 123182 Moscow, Russia.

†Present address: JINR, 141980 Dubna, Moscow region, Russia.

‡On leave from the Institute of Nuclear Physics, Krakow, Poland.

§Present address: RIKEN, Hirosawa 2-1, Wako, Saitama 351-0198, Japan.

[1] P. G. Young et al., Phys. Rev. **173**, 949 (1968).
[2] M. G. Gornov et al., Nucl. Phys. **A531**, 613 (1991).
[3] D. V. Aleksandrov et al., in Proceedings of the International Conference on Exotic Nuclei and Atomic Masses, (ENAM-95), Arles, France, 1995 (Editions Frontiers, Gif-sur-Yvette, France, 1995), p. 329.
[4] N. A. F. M. Poppelier et al., Phys. Lett. **157B**, 120 (1985).
[5] N. B. Shul'gina et al., Phys. Rev. C **62**, 014312 (2000).
[6] P. Descouvemont and A. Kharbach, Phys. Rev. C **63**, 027001 (2001).
[7] A. Sitenko and V. Tartakovski, Theory of Nucleus (Kluwer Academic Publishers, Dordrecht, 1997).
[8] G. E. Brown and A. D. Jackson, The Nucleon-Nucleon Interaction (North-Holland, Amsterdam, 1976).
[9] B. V. Danilin et al., Sov. J. Nucl. Phys. **53**, 45 (1991).
[10] M. Yasue et al., Nucl. Phys. **A510**, 285 (1990).
[11] S. A. Harbison et al., Nucl. Phys. **A152**, 503 (1970).
[12] D. V. Aleksandrov et al., JETP Lett. **62**, 18 (1995).